



APPLICATION OF FEED-FORWARD BACKPROPAGATION NEURAL NETWORK FOR THE DIAGNOSIS OF MECHANICAL FAILURES IN ENGINES PROVOKED IGNITION

APLICACIÓN DE UNA RED NEURONAL FEED-FORWARD BACKPROPAGATION PARA EL DIAGNÓSTICO DE FALLAS MECÁNICAS EN MOTORES DE ENCENDIDO PROVOCADO

Wilmer Contreras Urgilés^{1,*}, José Maldonado Ortega¹, Rogelio León Japa¹

Abstract

This research explains the methodology for the creation of a diagnostic system applied to the detection of mechanical failures in vehicles with gasoline engines through artificial neural networks. The system is based on the study of the intake phase of the Otto cycle, which is recorded through the physical implementation of a MAP sensor (Manifold Absolute Pressure). A strict sampling protocol and its corresponding statistical analysis are applied. Statistical values of the MAP sensor signal such as, area, energy, entropy, maximum, mean, minimum, power and RMS, were selected according to the greater amount of information and significant difference. The data were obtained with the application of 3 statistical methods (ANOVA, correlation matrix and Random Forest) to create a database that allows the training of a neural network feed-forward backpropagation, with which a classification error of 1.89×10^{-11} was achieved. The validation of the diagnostic system was carried out by the generating supervised failures in different engines with provoked ignition.

Keywords: diagnosis, mechanical failures, network feed-forward backpropagation, ANOVA, correlation matrix, Random Forest.

Resumen

En la presente investigación se explica la metodología para la creación de un sistema de diagnóstico aplicado a la detección de fallas mecánicas en vehículos con motores a gasolina mediante redes neuronales artificiales, el sistema se basa en el estudio de la fase de admisión del ciclo Otto, el cual es registrado a través de la implementación física de un sensor MAP (*Manifold Absolute Pressure*). Se emplea un estricto protocolo de muestreo y su correspondiente análisis estadístico. Los valores estadísticos de la señal del sensor MAP: área, energía, entropía, máximo, media, mínimo, potencia y RMS se seleccionaron en función al mayor aporte de información y diferencia significativa. Los datos se obtuvieron con la aplicación de 3 métodos estadísticos (ANOVA, matriz de correlación y Random Forest) para tener una base de datos que permita el entrenamiento de una red neuronal *feed-forward backpropagation*, con la cual se obtiene un error de clasificación de 1.89×10^{-11} . La validación del sistema de diagnóstico se llevó a cabo mediante la provocación de fallas supervisadas en diferentes motores de encendido provocado.

Palabras clave: diagnóstico, fallos mecánicos, red feed-forward backpropagation, ANOVA, matriz de correlación, Random Forest.

^{1,*}Research Group of Transportation Engineering (GIIT), Mechanical Engineer, Universidad Politécnica Salesiana Cuenca – Ecuador. Autor para correspondencia ✉: rcontreras@ups.edu.ec

<http://orcid.org/0000-0003-2300-9457>, <http://orcid.org/0000-0002-3846-2599>,

<http://orcid.org/0000-0003-2142-3769>

Received: 21-08-2018, accepted after review: 09-11-2018

Suggested citation: Contreras Urgilés, W.; Maldonado Ortega, J. and León Japa, R. (2019). «Application of feed-forward backpropagation neural network for the diagnosis of mechanical failures in engines provoked ignition». INGENIUS. N.°21, (january-june). pp. 32-40. DOI: <https://doi.org/10.17163/ings.n21.2019.03>.

1. Introduction

Nowadays, operators and technicians in the area of automotive transportation use rudimentary diagrams for diagnosing and repairing engines with provoked ignition (EPI), which implies subjectivity in the diagnosis, longer periods for fault detection, lack of assertiveness and, as a consequence, high maintenance costs.

Therefore, it becomes necessary to apply new methodologies and specialized techniques for quicker diagnosis, thus optimizing resources for fault detection in engines of gasoline powered vehicles [1].

Due to the complexity for analyzing and interpreting the operational parameters of the EPI, it is necessary to use neural networks and computational mathematics for an efficient diagnosis of mechanical failures in Otto cycle engines. Howlett [2] shows that the EPI can be monitored for failure diagnosis or control, by analyzing the spark plug signal using artificial neural networks.

Similarly, Antory [3] suggests that it is possible to precisely determine different types of common failures in automobile diesel engines, by means of a diagnosis model that uses a variation of autoassociative neural networks (AANN).

Other neural networks have also been applied for fault diagnosis in the automotive area. Chen and Zhao [4] use radial basis functions neural networks (RBFNN) to diagnose failures of the engine fuel system.

Parallel strategies can be applied to train an artificial neural network (ANN), e.g. training of a modified Elman network for diagnosing engine failures. This recurrent network can be very effective and achieve a good diagnosing result, due to its dynamic input-output relationship [5]. Similarly, Lian *et al.* [6] present a method based in fuzzy logic and neural networks, for diagnosing faults in engines with provoked ignition.

Shah *et al.* [7] propose a system for failure recognition of internal combustion engines, applying the discrete wavelet transform (DWT) and RBF neural networks. Cay [8] developed an ANN model based on the backpropagation algorithm, for predicting specific brake fuel consumption, effective power and exhaust temperature of an EPI. Cay *et al.* [9] presented an ANN model for predicting the performance and the exhaust emissions of an EPI working with methanol and gasoline.

There have been diverse applications of neural networks in the calibration of spark ignited engines. R. F. Turkson *et al.* [10] have stated that ANN are capable of identifying the system for rapid prototyping, virtual detection, emerging control strategies and on board diagnostic (OBD) applications.

Another important application of ANN with kinetic models as activation functions of units in the hidden layer, was the study of the polyurethane degradation of an automotive intake manifold with isothermal treatment [11].

The proposed system for diagnosing engines with provoked ignition can detect faults that are not detected by the engine control unit (ECU). The system uses the signals from the manifold absolute pressure (MAP) and camshaft positioning (CMP) sensors, since they can enable minimizing the diagnosis time, in order to avoid employing intrusive techniques in the EPI such as using manometers for measuring the compression of the cylinders and the fuel pressure, vacuum meter, scanner, among others. The purpose of the aforementioned techniques is determining mechanical failure.

2. Materials and methods

This section discusses subjects such as the selection of the minimally invasive experimental unit and instrumentation, conditions for samples collection, methodology for data acquisition, obtaining the matrix of attributes, reduction of attributes and selection for ANN training, and Matlab algorithm for implementing the neural network.

2.1. Selection of the minimally invasive experimental unit and instrumentation

The main purpose is to avoid disassembling elements and pieces of the engine when diagnosing mechanical failures, for which a MAP sensor is installed in a vacuum outlet of the intake manifold to measure engine depression. The sensor will be placed after the acceleration butterfly, to prevent the connection from affecting the engine operation.

The identification of each cylinder is carried out using the registered signal from the CMP sensor. Figure 1 shows the experimental unit tested in the engine of a Hyundai Sonata 2.0 DOHC, a personal computer (PC), a tablet, the data acquisition tool NI DAQ-6009 and the interface of an automotive scanner. On the other hand, Figure 2 shows the connection of the MAP sensor, the vacuum outlet and the Ni DAQ-6009.



Figure 1. Engine instrumentation.



Figure 2. Connection of the MAP sensor.

2.2. Conditions for samples collection

The software LabView 2017 and the data acquisition card NI DAQ-6009 were used for collecting the samples. The samples are taken with the engine idle, at approximately 850 rpm, for a temperature range of the MAP sensor between 92 °C y 97 °C and 40 % load; these conditions were confirmed using the scanner.

In a preliminary experimental study it was found that the signal of the MAP sensor exhibits higher frequency peaks. As a consequence, each signal was sampled at a frequency of 10 KHz during a period of 5 seconds; such frequency exceeds Nyquist criterion (1.416 KHz).

2.3. Methodology for data acquisition

Figure 3 presents the physical elements required for sampling the signals.

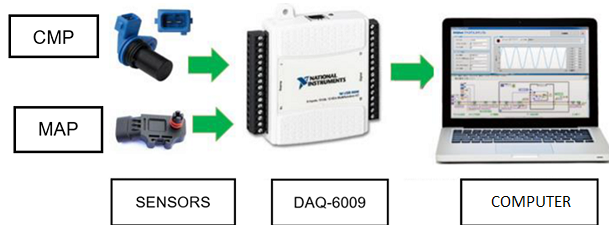


Figure 3. Elements required for collecting the samples.

The flowchart shown in Figure 4 represents the procedure for obtaining the data from the signals of the MAP and CMP sensors, with the engine operating correctly (Figure 4(a)) or under a supervised failure (Figure 4(b)). Such procedure starts with the revision of the engine to determine its condition.

Then, the connection of the sensors is verified and the signal is recorded with the software LabView and saved to an Excel file.

Table 1 summarizes a total of 18 failures that can occur in the experimental unit, each with its corresponding identification code. The optimal operation of the engine is also included as a condition.

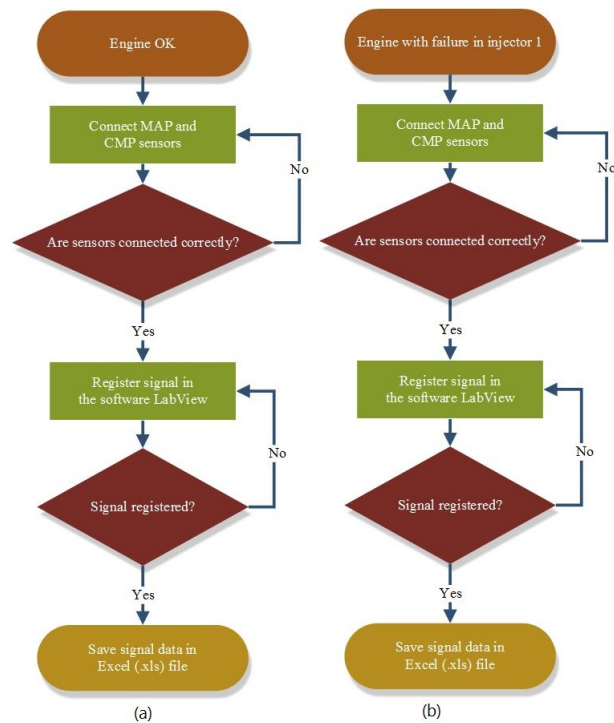


Figure 4. Flowchart of the procedure for data acquisition: (a) engine operating correctly, (b) engine with a failure

Table 1. Operational conditions of the experimental unit

N.º	Type of mechanical condition	Identification Code
1	Optimal operation	100
2	Failure in fuel injector 1	200
3	Failure in fuel injector 2	300
4	Failure in fuel injector 3	400
5	Failure in fuel injector 4	500
6	Failure in spark plug 1	600
7	Failure in spark plug 2	700
8	Failure in spark plug 3	800
9	Failure in spark plug 4	900
10	Failure in coil 1-4	1000
11	Failure in coil 2-3	1100
12	Low fuel pressure	1200
13	High fuel pressure	1300
14	Intake (+1) and exhaust (0) trees	1400
15	Intake (-1) and exhaust (0) trees	1500
16	Intake (0) and exhaust (+1) tree	1600
17	Intake (0) and exhaust (-1) trees	1700
18	Intake (+1) and exhaust (+1) trees	1800
19	Intake (-1) and exhaust (-1) trees	1900

2.4. Obtaining the matrix of attributes

Once the signals have been acquired, an algorithm was coded in Matlab for reading and obtaining the matrix with general attributes, such as geometric mean, maximum, minimum, covariance, variance, standard deviation, mode, kurtosis factor, coefficient of asymmetry, energy, power, area under the curve, entropy,

coefficient of variation, range, root mean square and crest factor.

Figure 5 illustrates a complete cycle of the engine ($720^\circ \pm 180^\circ$), with the tuning of the early intake opening (EIO) and late intake closing (LIC) distribution for each cylinder. Figure 6 shows windows of the MAP sensor signal for each cylinder; these signals are characterized.

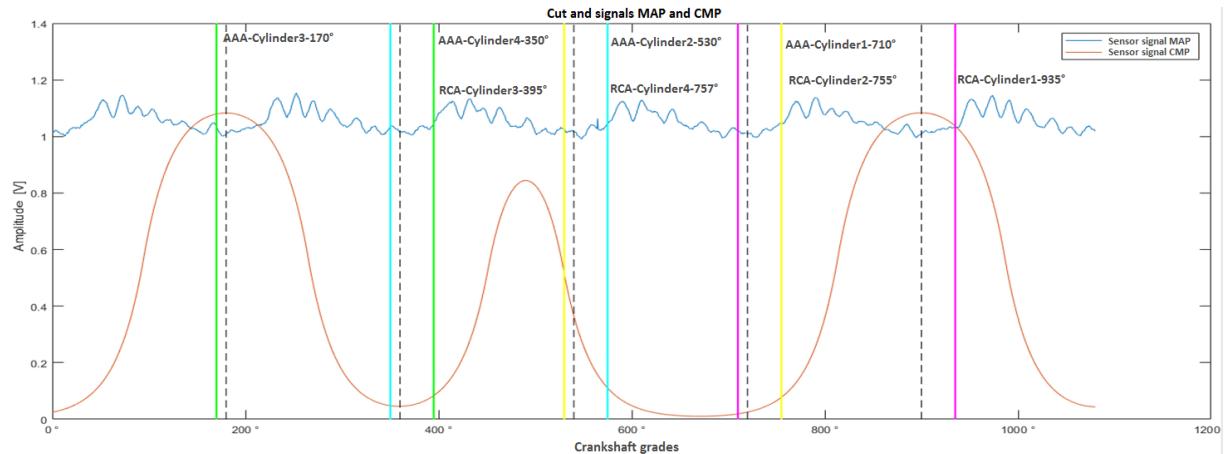


Figure 5. Signals of the MAP and CMP sensors.

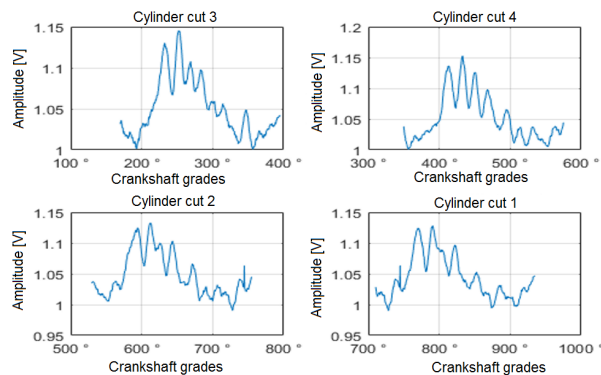


Figure 6. Windows of the MAP sensor signal for each cylinder.

2.5. Reduction of attributes

For selecting and reducing the number of attributes, the general matrix is analyzed using three statistical methods: analysis of variance (ANOVA), correlation matrix and Random Forest.

The application of a single factor ANOVA to all 18 attributes, helps to determine the best attributes that will be present in the general matrix. Since values of R^2 close to 100 % indicate a correct fit of the model to the data, greater values of this parameter are used to determine the variation among the attributes. In addition, values of p close to 0 determine if the attributes are statistically significant [12].

With respect to the correlation matrix, attributes with coefficients close to -1 or 1 were discarded, since such values indicate strong relationship between the variables, either negative (-1) or positive (1). In fact, attributes with coefficients close to zero were selected, because there does not exist strong correlation between the variables [13].

Regarding the Random Forest method, it was used to estimate the importance of the attributes by means of techniques such as Curvature test, Standard CART and Interaction test. Then, Pareto analysis was applied to select the attributes with the higher priority, considering only the first 95 % of the accumulated distribution [14].

Table 2 contains the results of the applied statistical methods, i.e. ANOVA, correlation matrix and Random Forest.

The general matrix contains the 18 attributes corresponding to the 19 conditions which were induced in the experimental unit.

2.6. Selection of attributes for training the ANN

The attributes selected for training the neural network were the most often repeated, which were determined by means of a coincidence analysis carried out to the results of Table 2. The selected attributes are shown in Table 3, thus confirming the effectiveness of each method.

Table 2. General matrix of attributes

Statistical methods	Most important attributes according to the statistical methods								
Analyzed Correlation coefficients 342	Coeff. of variation Range/value $\leq \pm 0.1 / 222$	Area Range/value $\leq \pm 0.1 / 212$	RMS Range/value $\leq \pm 0.1 / 216$	Mean Range/value $\leq \pm 0.1 / 212$	Energy Range/value $\leq \pm 0.1 / 220$	Entropy Range/value $\leq \pm 0.1 / 214$	Minimum Range/value $\leq \pm 0.1 / 204$	Median Range/value $\leq \pm 0.1 / 214$	Power Range/value $\leq \pm 0.1 / 214$
ANOVA $R^2=100\%$ $p=0,00$	Median $R^2=99,4\%$ $p=0,00$	Area $R^2=99,39\%$ $p=0,00$	Mean $R^2=99,39\%$ $p=0,00$	Minimum $R^2=99,38\%$ $p=0,00$	Maximum $R^2=99,38\%$ $p=0,00$	RMS $R^2=99,26\%$ $p=0,00$	Power $R^2=99,25\%$ $p=0,00$	Energy $R^2=99,25\%$ $p=0,00$	Entropy $R^2=99,16\%$ $p=0,00$
Forest Curvature % of Importance (0 a 2,5)	Energy % Imp. 2,4	RMS % Imp. 2,3	Entropy % Imp. 2,25	Maximum % Imp. 2,2	Area % Imp. 2,18	Mean % Imp. 2,15	Power % Imp. 2	Minimum % Imp. 1,9	Crest factor % Imp. 1,6
Forest Standard Cart % of Importance (0 a 3)	Energy % Imp. 2,85	Entropy % Imp. 2,7	RMS % Imp. 2,65	Mean % Imp. 2,64	Maximum % Imp. 2,63	Area % Imp. 2,6	Power % Imp. 2,55	Minimum % Imp. 2,46	Coeff. of variation % Imp. 2,4
Forest Robust % of Importance (0 a 12)	Standar Deviation % Imp. 10,15	Variance % Imp. 10,13	Energy % Imp. 10,11	Area % Imp. 10,09	RMS % Imp. 9,5	Mean % Imp. 9,1	Power % Imp. 8,7	Maximum % Imp. 8,5	Minimum % Imp. 8,4

Table 3. Attributes used to train the ANN

Statistical attributes	Number of repetitions
Area (v^2)	5
Energy (J)	5
Entropy (J)	4
Maximum (V)	4
Mean (V)	5
Minimum (V)	5
Power (mW)	5
RMS (V)	5

2.7. Matlab algorithm for implementing the neural network

Different network configurations were created and trained using the Matlab neural network toolbox, in the search for the network that exhibits good generalization ability.

Figure 7 shows the flow chart of the procedure for creating an ANN.

The procedure starts reading the matrix of inputs and target data for the ANN. Then, for better training performance, the data is normalized using the corresponding maximum values. At last, the ANN is created.

Figure 8 illustrates the structure of the feed-forward backpropagation ANN.

Once created, the neural network is trained considering the following training parameters:

1. Training algorithm
2. Number of epochs
3. Maximum error

Then, the classification performance of the trained neural network is tested. Is the classification error is greater than 5 %, the parameters are varied and the training is repeated.

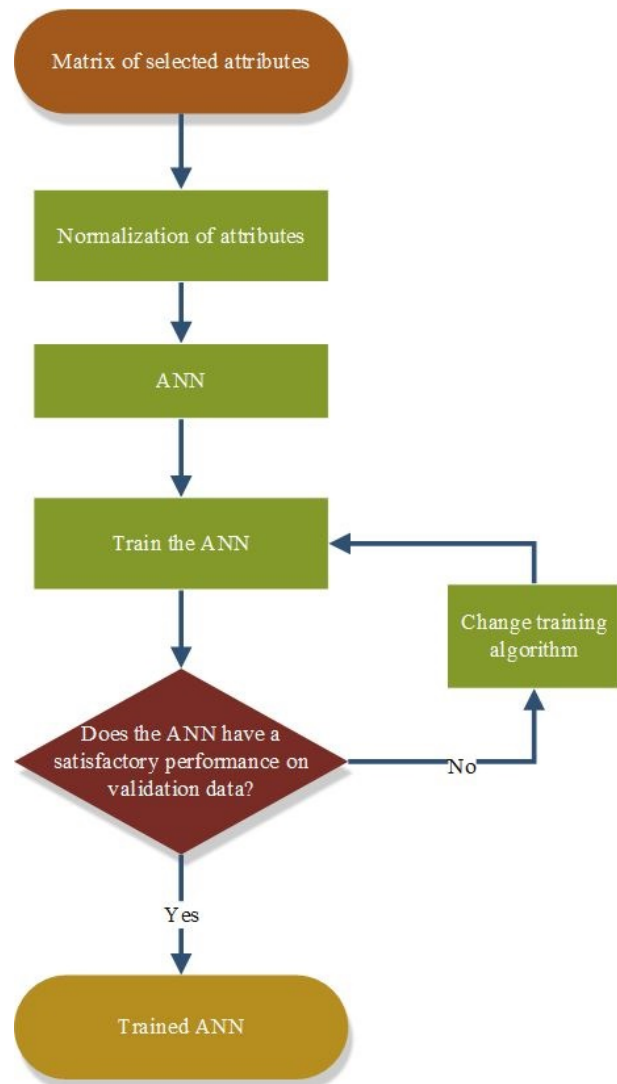
**Figure 7.** Flowchart of the procedure for ANN creation

Figure 9 shows the classification error of different training configurations, which were carried out searching for the neural network with the smallest possible error.

The neural network trained with the function trainscg had an error of $1.89e^{-11}$ %.

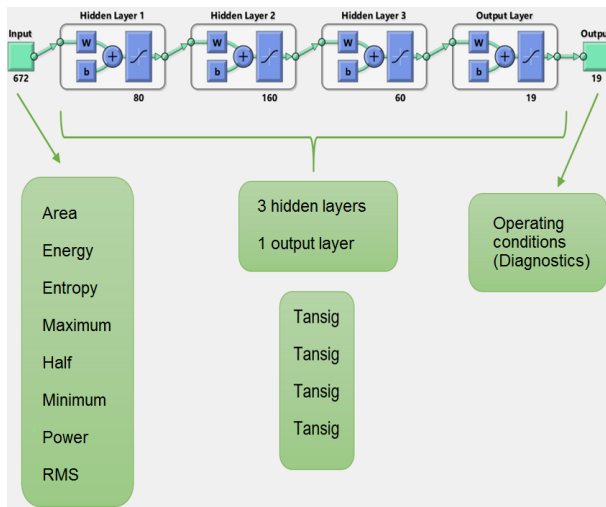


Figure 8. Structure of the neural network.

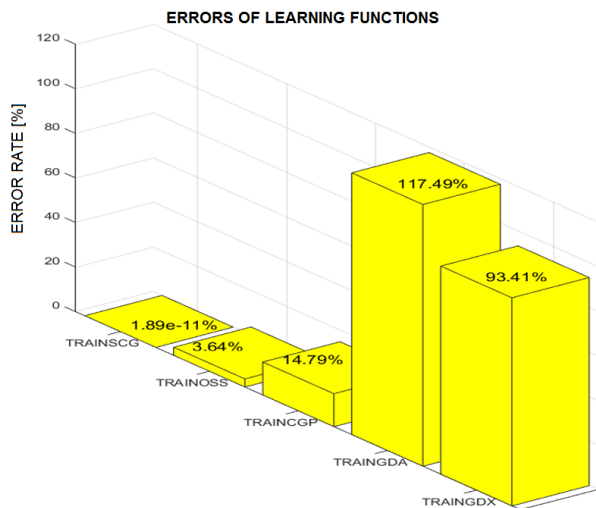


Figure 9. Errors for different training algorithms.

Figure 10 shows the Pearson correlation coefficient R of the created neural network, which is available in the Matlab string variable `red.trainFcn = 'trainscg'`.

The lines represent target values and the black circles the corresponding values estimated by the ANN. The neural network exhibits a good performance, since $R=1$ for training, validation and testing, which indicates a strong linear relationship between the real conditions of the EPI and the results given by the neural network [15].

On the other hand, Figure 11 shows a comparison between the output of the neural network and the target value, for the 19 mechanical conditions under consideration.

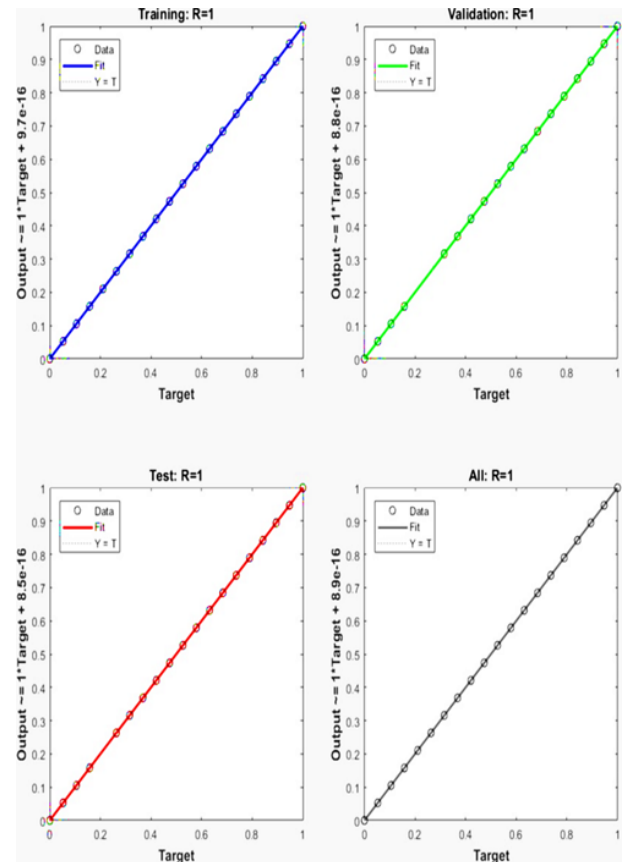


Figure 10. Correlation between the targets and the values estimated by the neural network.

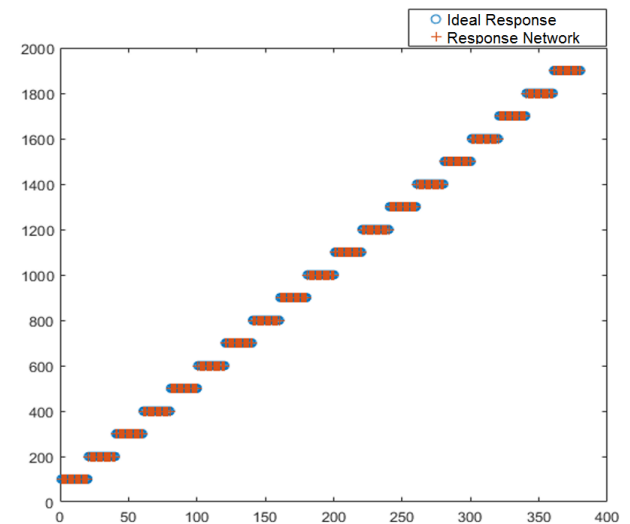


Figure 11. The Neural network trained with function «trainscg» achieved a percentage error of $1.89e^{-11}$.

3. Results and discussion

Tests under different operating conditions were conducted to confirm that the proposed diagnosing system works correctly.

Specifically, two failure conditions were considered: injector 1 (200) and coil 2-3 (1100).

Figure 12 shows the results for a failure condition in injector 1. The average error between the target values and the outputs of the neural network was 0.0127.

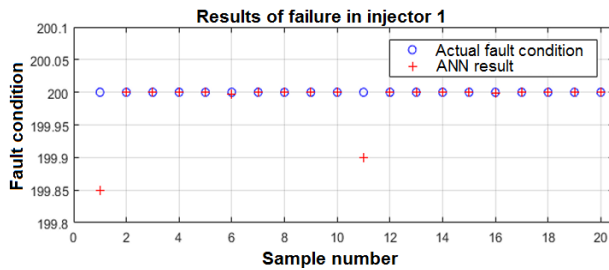


Figure 12. Results for a failure condition in injector 1.

On the other hand, Figure 13 shows the results for the failure condition in coil 2-3. The average error between the target values and the outputs of the neural network was 0.0060.

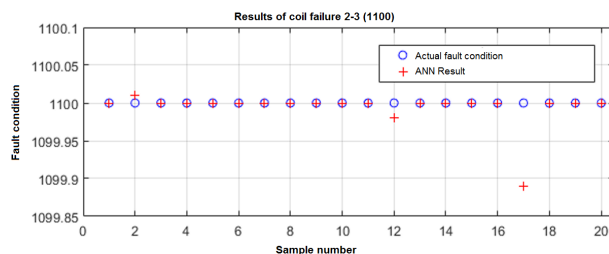


Figure 13. Results for a failure condition in the ignition coil 2-3.

Results show that the differences between the target values and the outputs of the ANN were very close to zero. Therefore, the proposed diagnosing system is capable of detecting a real failure condition.

In fact, Figure 14 shows that Tukey statistical method with a confidence interval of 95 %, determines that there is not significant statistical difference between the real condition of the engine and the responses of the ANN, since their means are equivalent.

In addition, the intervals shown in Figure 15 indicate that there is no difference between the average values of the tests in the different operating conditions of the engine.

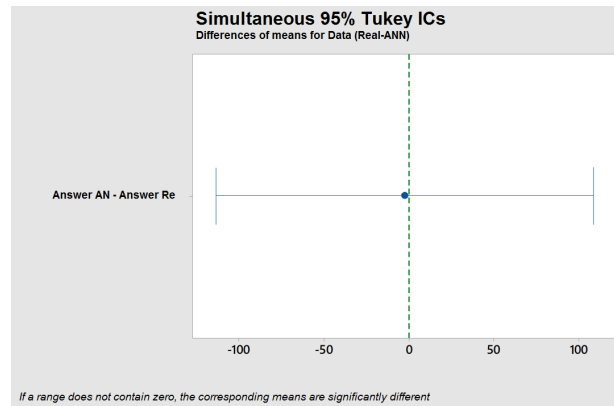


Figure 14. Difference between the means of the real data vs. ANN response.

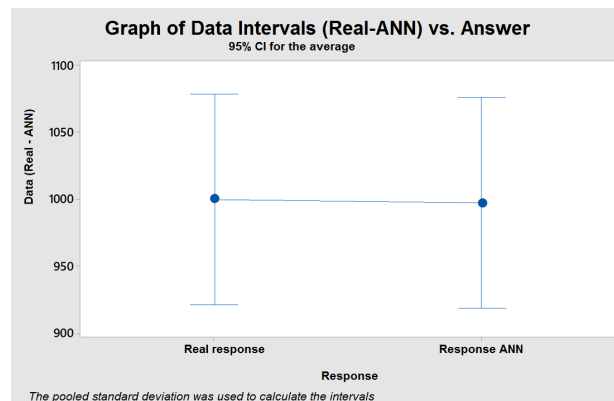


Figure 15. Intervals of real data vs. ANN response.

Similarly, Figure 16 confirms that there is relationship between the expected and neural network responses, since they share the same group letter (A) and the p-value is 0.965. This results in a confidence value of 96.5 %, which is very acceptable in the diagnosis of internal combustion engines with provoked ignition.

Variance analysis

Source	GL	SC Adjust.	MC Adjust.	Value F	Value p
Response	1	597	597	0,00	0,965
Error	378	114792201	303683		
Total	379	114792798			

Comparisons in pairs of Tukey

Group information using the Tukey method and a confidence of 95%

Response	N	Media Grouping
Real response	190	1000,0 A
ANN response	190	997,5 A

Figure 16. Results of the analysis of variance and comparisons in Tukey pairs.

4. Conclusions

The developed neural network model had a classification error of 1.89×10^{-11} with the training function `trainscg`, which yielded an accurate identification of the different types of mechanical conditions of the EPI. Therefore, such model constitutes a completely viable alternative to be integrated in a diagnosing system, due to the high computational speed offered by the artificial neural networks.

By means of a single factor analysis of variance, a p -value=0,965 was obtained, demonstrating that the targets and the ANN responses are equivalent since this p -value indicates that there is not a significant statistical difference between them. This work showed that feed-forward backpropagation neural networks are suitable for detecting mechanical failure conditions in engines with provoked ignition; in addition, the applied diagnosing technique has the advantage of avoiding disassembling elements and pieces of the engine, thus being a reliable and highly precise minimally invasive technique.

Statistical methods such as analysis of variance (ANOVA), correlation matrix and Random Forest, were applied to determine the best attributes for training the ANN. Then, the results were grouped in a general matrix, to help in the selection of the attributes with greater coincidence and importance for differentiating patterns of mechanical failures.

References

- [1] W. Contreras, M. Arichávala, and C. Jerez, "Determinación de la presión máxima de compresión de un motor de encendido provocado basado en una red neuronal artificial recurrente," *INGENIUS*, no. 19, pp. 9–18, 2018. [Online]. Available: <http://doi.org/10.17163/ings.n19.2018.01>.
- [2] R. J. Howlett, "Condition monitoring and fault diagnosis in a domestic car engine using a neural network," in *IEE Colloquium on Artificial Intelligence in Consumer and Domestic Products (Digest No. 1996/212)*, Oct 1996, pp. 5/1–5/4. [Online]. Available: <https://doi.org/10.1049/ic:19961142>
- [3] D. Antory, "Fault diagnosis application in an automotive diesel engine using auto-associative neural networks," in *International Conference on Computational Intelligence for Modelling, Control and Automation and International Conference on Intelligent Agents, Web Technologies and Internet Commerce (CIMCA-IAWTIC'06)*, vol. 2, Nov 2005, pp. 109–116. [Online]. Available: <https://doi.org/10.1109/CIMCA.2005.1631454>
- [4] D. Chen and P. Zhao, "Study of the fault diagnosis method based on rbf neural network," in *2011 2nd International Conference on Artificial Intelligence, Management Science and Electronic Commerce (AIMSEC)*, Aug 2011, pp. 4350–4353. [Online]. Available: <https://doi.org/10.1109/AIMSEC.2011.6010128>
- [5] Y. G. Wu, C. Z. Song, and L. P. Shi, "Notice of retraction fault diagnosis of engine mission using modified elman neural network," in *2010 Sixth International Conference on Natural Computation*, vol. 2, Aug 2010, pp. 996–998. [Online]. Available: <https://doi.org/10.1109/ICNC.2010.5582900>
- [6] P. Lian, T. Y. Bin, N. Ning, and C. Aiping, "Application of fuzzy neural network in fault diagnosis of gasoline engine," in *2009 9th International Conference on Electronic Measurement Instruments*, Aug 2009, pp. 4–602–4–605. [Online]. Available: <https://doi.org/10.1109/ICEMI.2009.5274658>
- [7] M. Shah, V. Gaikwad, S. Lokhande, and S. Borhade, "Fault identification for i.c. engines using artificial neural network," in *2011 International Conference on Process Automation, Control and Computing*, July 2011, pp. 1–6. [Online]. Available: <https://doi.org/10.1109/PACC.2011.5978891>
- [8] Y. Cay, "Prediction of a gasoline engine performance with artificial neural network," *Fuel*, vol. 111, pp. 324–331, 2013. [Online]. Available: <https://doi.org/10.1016/j.fuel.2012.12.040>
- [9] Y. Çay, I. Korkmaz, A. Çiçek, and F. Kara, "Prediction of engine performance and exhaust emissions for gasoline and methanol using artificial neural network," *Energy*, vol. 50, pp. 177–186, 2013. [Online]. Available: <https://doi.org/10.1016/j.energy.2012.10.052>
- [10] R. F. Turkson, F. Yan, M. K. A. Ali, and J. Hu, "Artificial neural network applications in the calibration of spark-ignition engines: An overview," *Engineering Science and Technology, an International Journal*, vol. 19, no. 3, pp. 1346–1359, 2016. [Online]. Available: <https://doi.org/10.1016/j.jestch.2016.03.003>
- [11] B. D. de L. Ferreira, N. R. Araújo, R. F. Ligório, F. J. Pujatti, M. I. Yoshida, and R. C. Sebastião, "Comparative kinetic study of automotive polyurethane degradation in non-isothermal and isothermal conditions using artificial neural network," *Thermochimica Acta*, vol. 666, pp. 116–123, 2018. [Online]. Available: <https://doi.org/10.1016/j.tca.2018.06.014>
- [12] Minitab. (2018) Minitab software. [Online]. Available: <https://goo.gl/ND0MT0>

- [13] Incibe-cert. (2015) Incibe-cert. [Online]. Available: <https://goo.gl/5h7696>
- [14] Mathworks. (2018) Mathworks. [Online]. Available: <https://goo.gl/GVhckj>
- [15] J. Calderón, B. Castillo, and J. Moreno, “Diseño de una red neuronal para la predicción del coeficiente de pérdidas primarias en régimen de flujo turbulento,” *INGENIUS*, vol. 20, pp. 21–27, 2018. [Online]. Available: <https://doi.org/10.17163/ings.n20.2018.02>.